

# CoMo/Al<sub>2</sub>O<sub>3</sub>-MgO Supported Catalysts: Improvement of Hydrodesulfurization Activity and Optimization of Operational Processing

X. G. Zheng<sup>1</sup> and Y. Y. Yue<sup>1\*</sup>

<sup>1</sup> National Engineering Research Center of Chemical Fertilizer Catalyst, School of Chemical Engineering, Fuzhou University, Fuzhou 350002, China

Received 20 February 2022; revised 30 March 2022; accepted 23 April 2022; published online 06 May 2022

**ABSTRACT.** Hydrodesulfurization (HDS) plays a vital role in the production of clean fuels when more stringent environmental legislation forces the sulfur content in fuels to an ultra-low level. There are two alternative approaches for producing ultra-low sulfur diesel (ULSD) in a cost-effective way, including the activity improvement of HDS catalysts and the optimization of the operating conditions in HDS reactions. In this study, the activity improvement of HDS catalysts was first examined, and then the optimization of operational conditions was further explored to gain the ULSD in a cost-effective way. In detail, the catalysts were improved through optimizing the ratio between active metal (Mo) and promoter (Co) based on the MgO-Al<sub>2</sub>O<sub>3</sub> as support. Precursors of the improved oxide catalysts and sulfide catalysts were characterized by various techniques, and the catalytic performances were further evaluated in the hydrodesulfurization of dibenzothiophene. Catalysts with the best catalytic performance were chosen to optimize the reaction conditions. Results show that the optimal amounts of catalysts were 4 wt.% of MoO<sub>3</sub> and combined with 2 wt.% of CoO. Moreover, the optimal reaction conditions were reaction temperature of 240 °C, total reaction pressure of 4.0 MPa, the hydrogen-to-oil volume ratio of 300, and LHSV of 2.0 h<sup>-1</sup>. Under the optimal reaction condition, the desulfurization rate could reach to 99.8%.

**Keywords:** Al<sub>2</sub>O<sub>3</sub>-MgO supported catalysts, optimization, hydrodesulfurization, CoMoS, dibenzothiophene

## 1. Introduction

Refiners are facing challenges to offer clean-transportation fuels to meet the growing demand for environmental regulations (Topsøe et al., 1996; Song, 2003; Fujikawa et al., 2006). Particularly, sulfur in diesel fuels is now strongly desired to be removed since it is adverse to the durability of catalytic converter for exhaust-emission treatment (Fujikawa et al., 2006). Consequently, environment specifications have been implemented in many countries around the world to reduce the sulfur content of diesel fuel to very low levels (ULSD, < 10 ppm sulfur) to decrease pollution of diesel engines and improve air quality (Ho, 2004; Kouzu et al., 2004; Hamiye et al., 2017). For example, sulfur contents in diesel fuels in the United States were required to be below 10 ppm in 2008 (Oyama et al., 2009); in 2011, sulfur content standards mandate to under 10 ppm in the European Union (Li, 2016); similar sulfur-level requirements were legislated as well in China and Japan (Fujikawa et al., 2006; Ke and Wang, 2016). Since the removal of sulfur compounds in diesel fractions has become extremely necessary due to the demands for ULSD fuels, fuel industry is eager to further improve the catalytic performance of HDS catalysts and

optimize HDS process conditions in terms of the refractory sulfuric constituents such as dibenzothiophene (DBT).

Catalysts are widely considered as the key factor of the HDS process and transition metal sulfide (TMS) catalysts have been the principal HDS catalysts employed in refineries (Eijbsbouts et al., 2007). In detail, these catalysts are composed of Mo or W-sulfides with catalytical activity promoted by the sulfides of Co or Ni. Additionally, widespread works have been devoted to analyzing HDS effects of the TMS catalysts (Vissenberg et al., 2001; Zuo et al., 2004; Hensen et al., 2007; Peñaer et al., 2014). There are extensive studies related to molybdenum-based catalysts used in HDS (Lauritsen et al., 2001). In contrast, fewer papers are associated with the applications of tungsten-based catalysts. Although the structure of WS<sub>2</sub> looks similar to that of MoS<sub>2</sub>, it is more difficult to convert tungsten oxide to WS<sub>2</sub> than molybdenum oxide to MoS<sub>2</sub> (Sun et al., 2004). Owing to the synergetic effect, Mo-based catalysts with the addition of Co or Ni are inferred to be far more active in the HDS process than unpromoted catalysts, while the incorporation of Co in W-based catalysts have no such an effect (Lauritsen et al., 2007). Consequently, a catalytic process commonly performs on Co-promoted Mo-based catalysts. Besides, these catalysts typically are commonly confirmed that promoter atoms (Co) occupy the edges of MoS<sub>2</sub> nanoparticles, as described in the so-called CoMoS model (Topsøe et al., 1981). These promoted sites are gained by

\* Corresponding author. Tel.: 86 0591 22865220; fax: 86 0591 22865220. E-mail address: yueyy@fzu.edu.cn (Y. Y. Yue).

sulfidation of oxide precursors and are considered as the active sites in HDS reactions (Hamiye et al., 2017).

Not only active metal but also support largely affect the number of HDS catalysts' active sites (Trejo et al., 2008). Commonly, supports of HDS catalysts are alumina-based (Hensen et al., 2002). The combination of MgO, SiO<sub>2</sub>, TiO<sub>2</sub>, ZrO<sub>2</sub> with Al<sub>2</sub>O<sub>3</sub> would alter the interaction between active phase and support (Rana et al., 2005; Trejo et al., 2008). Therefore, these oxides play a structural promoting position to the support contribution and its interaction towards the active metal (Ancheyta et al., 2005; Trejo et al., 2008). Among these oxides, MgO-Al<sub>2</sub>O<sub>3</sub> could improve the interaction between support and acidic molybdenum species (MoO<sub>3</sub>) due to basicity of MgO (Klimova et al., 1998; Klicpera and Zdražil, 2002; Breyse et al., 2003a, b; Caloch et al., 2004; Trejo et al., 2008). Consequently, MgO-Al<sub>2</sub>O<sub>3</sub> as support applied in HDS catalysts can show a wide range of textural properties and improve catalytic performance.

Apart from the theoretical studies of the HDS catalysts, optimization of HDS process conditions has also attracted much attention in order to achieve ultra-deep HDS of diesel fuel without new investment in petroleum refineries. It is helpful to remove the sulfur content contained in diesel fuel by modifying operating conditions for HDS reactions, including the reaction temperature, reaction pressure, reaction hydrogen-to-oil (H/Oil) volume ratio, and reaction liquid hourly space velocity. In general, higher reaction temperature results in coke formation on the catalyst and rapid catalytic deactivation; higher reaction pressure requires more rigorous equipment, resulting in increase of investment; higher H/Oil volume ratio needs more hydrogen and causes increase of reaction cost; lower LHSV results in reduced hydrotreating efficiency, requiring an additional reactor or replacement of a larger reactor (Fujikawa et al., 2006). Consequently, other than developing a catalyst, the best way of achieving the ultra-deep HDS in a cost-effective manner is to optimize the operation condition of the HDS reaction.

Therefore, as an extension of the previous efforts, the objective of this research is not only to improve the HDS catalysts but also optimize the process conditions of HDS in order to achieve the ULSD fuels under the minimization of the HDS-reaction cost. In our previous study, MgO-Al<sub>2</sub>O<sub>3</sub> support was synthesized using the composite oxides of MgAl-hydrotalcite and alumina, and catalysts with MgO-Al<sub>2</sub>O<sub>3</sub> as support were found to have high activity in the HDS of diesel fuels (Yue et al., 2018). In this research, the HDS catalysts are improved by optimizing the amounts of active metal (Mo) and promoter (Co) based on the MgO-Al<sub>2</sub>O<sub>3</sub> as support. Moreover, several characterizations with multi methods, including XRD, N<sub>2</sub> adsorption-desorption, NH<sub>3</sub>-TPD, H<sub>2</sub>-TPR, and XPS, as well as catalytic tests were carried out, and were used to correlate the physicochemical properties with the activities. After the best amounts of Co and Mo are verified, the operation conditions of HDS are then optimized to obtain the optimal reaction conditions.

## 2. Experimental Section

### 2.1. Materials

The 65 ~ 68% nitric acid (HNO<sub>3</sub>) was acquired from Xilong Chemical Co., Ltd. (P. R. China). Ammonium heptamolybdate and Cobalt Nitrate Hexahydrate were purchased from Sino-pharm Chemical Reagent Co., Ltd. (P. R. China). *n*-heptane and Cyclohexane were obtained from Tianjin Zhiyuan Chemical Reagent Co., Ltd. (P. R. China). Dibenzothiophene (DBT) was purchased from Zhengzhou Haikuo Photoelectric Material Co., Ltd. (P. R. China). Aluminum hydroxide dry glue was gained from Shandong Xindu Petrochemical Co., Ltd. (P. R. China). Tian Jing power was taken from Lankao Country Plant Glue Factory. (P. R. China). Magnesium-aluminum hydrotalcite (MgAl-LDHs) was acquired from Jingjiang Kanggaote Plastic Co., Ltd. (P. R. China).

### 2.2. Synthesis of Catalysts

In this study, a series of CoMo/Al<sub>2</sub>O<sub>3</sub>-MgO catalysts were prepared by using the composite oxides of MgAl-LDHs and alumina as supports via an incipient-wetness impregnation method. The synthesis-method details are described in the following sub-sections.

#### 2.2.1. Preparation of Al<sub>2</sub>O<sub>3</sub>-MgO supports

The magnesium-aluminum hydrotalcite (MgAl-LDHs) with a magnesium-aluminum molar ratio of 3 was first calcined at 800 °C for 4 hours, and the obtained sample was recorded as a magnesium-aluminum composite oxide (MgAl-LDO). Subsequently, MgAl-LDO and aluminum hydroxide dry adhesive were mixed at a mass ratio of 1:9. Meanwhile, a suitable amount of Tianjin powder and nitric acid solution were added. Afterward, extruding materials with 2.0 mm cylindrical can be gained using a double screw bar extruding machine. Lastly, extruding materials were dried at 80 °C for 12 hours and calcined at 520 °C for 4 hours to obtain Al<sub>2</sub>O<sub>3</sub>-MgO support with a length of 2 ~ 4 mm.

#### 2.2.2. Preparation of Al<sub>2</sub>O<sub>3</sub>-MgO-supported CoMo catalysts

An incipient-wetness impregnation method was employed to gain Al<sub>2</sub>O<sub>3</sub>-MgO-supported CoMo catalysts. A certain amount of Ammonium Heptamolybdate (AH) was first dissolved in dilute ammonia solutions, then a certain amount of cobalt nitrate hexahydrate (CNH) was added after AH was completely dissolved. After CNH was completely dissolved, the metal-containing salt solution was dropped on prepared strip-shaped supports, as well as completely immersed. Finally, a series of CoMo/Al<sub>2</sub>O<sub>3</sub>-MgO catalysts were obtained by drying at 80 °C for 5 hours and calcining at 520 °C for 4 hours, named MC-*xy* (*x* represents the mass content of loaded MoO<sub>3</sub>, and *y* represents the mass content of loaded CoO)

### 2.3. Characterizations

The phase structure of CoMo/Al<sub>2</sub>O<sub>3</sub>-MgO catalysts were determined by X-ray power diffraction (XRD) on a PANalytical

X'pert Pro diffractometer with Cu K $\alpha$  radiation and operated at 40 kV and 40 mA in the  $2\theta$  range of  $5 \sim 50^\circ$ . The textural properties of the samples were studied by nitrogen (N<sub>2</sub>) adsorption-desorption measurements at  $-196^\circ\text{C}$  on an ASAP 2020 M Micromeritics instrument (U.S.A.). The specific surface areas were calculated by the Brunauer-Emmett-Teller (BET) method, and the specific micropore surface areas and pore volumes were obtained by the t-plot method. The BJH pore size model was employed to obtain the mesopore size distribution using the adsorption branch of the isotherm.

The acidity of the samples was measured by temperature-programmed desorption of ammonia (NH<sub>3</sub>-TPD) on an AutoChem 2920 apparatus equipped with a thermal conductivity detector (TCD). In addition, the reducibility of samples could be determined by H<sub>2</sub>-programmed temperature reduction (H<sub>2</sub>-TPR) on an AutoChem 2920 apparatus equipped with a thermal conductivity detector (TCD).

The X-ray photoelectron spectra (XPS) of the catalysts were measured on ESCA Lab 250 using monochromated Al K $\alpha$  radiation (0.5 eV). Spectra were recorded with a constant pass energy of 285.0 eV. The sulfurized degree of catalysts can be calculated by analyzing the XPS spectrum of Mo 3d when the active metal loading was same (Wagner et al., 1979; Hensen et al., 2002; Qiu and Xu, 2010). In detail, the ratios of Mo<sup>6+</sup>, Mo<sup>5+</sup>, and Mo<sup>4+</sup> could be quantitatively calculated from the peak deconvolution of the Mo 3d spectrum. The binding energy of different valence states of Mo species is shown in Table 1, and sulfurized-degree formula of catalysts is presented in Equation (1) (Fan et al., 2011).

$$\text{Mo}_{\text{sulfidation}} = \text{Mo}^{4+}/(\text{Mo}^{4+} + \text{Mo}^{5+} + \text{Mo}^{6+}) \quad (1)$$

**Table 1.** The Binding Energy of Different Valence States of Mo Species

Binding energy	Mo <sup>4+</sup> (MoS <sub>2</sub> )	Mo <sup>5+</sup> (MoS <sub>x</sub> O <sub>y</sub> )	Mo <sup>6+</sup> (MoO <sub>3</sub> )
Mo3d <sub>5/2</sub>	229.1	230.5	232.8
Mo3d <sub>3/2</sub>	232.0	233.8	236.0

#### 2.4. Catalytic Tests

The HDS performance of catalysts was conducted in a 10 mL continuous flow fixed-bed microreactor (Length 574 mm, inner diameter 25.4 mm, outer diameter 10.0 mm) shown in Figure 1. The raw material was model compound with a 1 wt.% dibenzothiophene (DBT)/*n*-heptane solution. Firstly, the pre-sulfurization of the catalysts was carried out at  $360^\circ\text{C}$  for 5 h, with a CS<sub>2</sub> (3wt.%)/cyclohexane mixture as vulcanizer and hydrogen as carrier gas, a total pressure of 4.0 MPa, a hydrogen-to-oil (H/Oil) volume ratio of 300, and a liquid hourly space velocity (LHSV) of  $2.0\text{ h}^{-1}$ . Subsequently, the model compound was fed into the reactor by a microscale pump at a given flow rate, and the HDS reaction was carried out at a temperature of  $300^\circ\text{C}$ , a total pressure of 4.0 MPa, a H/Oil volume ratio of 300, and a LHSV of  $2.0\text{ h}^{-1}$ . At a constant time interval, the product was collected and analyzed with a trace sulfur analyzer (RPP-5000SN).

### 3. Results and Discussions

#### 3.1. Effect of Mo Content on the Performance of CoMo/Al<sub>2</sub>O<sub>3</sub>-MgO Catalyst

Impacts of Mo amount on the HDS performance of the

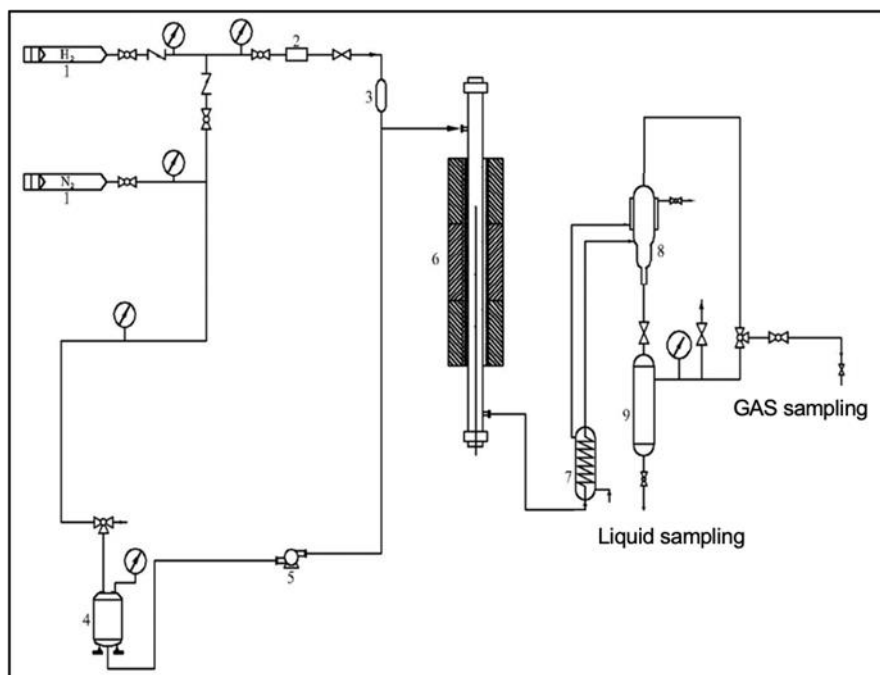


**Figure 1.** The device for catalyst evaluation (1-Gas bottle; 2-mass flow controller; 3-gas mixer; 4-feed tank; 5-liquid pump; 6-reactor and furnace; 7-compensator; 8-high pressure gas/liquid separator; 9-product tank).

CoMo/Al<sub>2</sub>O<sub>3</sub>-MgO catalyst are investigated with the same amounts of Co (2 wt.%). The obtained catalysts are named MC-32, MC-42, and MC-52, which represent 3, 4, and 5 wt.% of MoO<sub>3</sub>, respectively. In this section, the structure and pore properties of catalysts are analyzed, then the HDS reactions are conducted to help confirm the properties of catalysts.

### 3.1.1 Structure and Pore Properties of Catalysts with Various Mo Content

The phase structure of the synthesized catalysts with different Mo amount was determined by XRD, and the results are shown in Figure 2. There are six characteristic peaks which all belong to the  $\gamma$ -Al<sub>2</sub>O<sub>3</sub> phase (PDF#29-0063), including (111), (220), (311), (400), (511), and (440) crystal planes. It could be known that support is dominated by  $\gamma$ -Al<sub>2</sub>O<sub>3</sub>. Besides, there are also no characteristic diffraction peaks of MgO because the products of 10 wt.% MgAl-LDHs are completely converted into compounds of MgAl<sub>2</sub>O<sub>4</sub>, MgO and MgAlO after calcination at 800 °C. When metal dispersion is high, the formed crystal grains are too small to be detected by XRD. In contrast, if metal dispersion is low, large-size grains would be formed on the surface of the support and the characteristic peaks of bulk metal oxides could be found in the XRD pattern. Hence, MgO is dispersed well in the support. In Figure 2, the characteristic diffraction peaks of MoO<sub>3</sub> and CoO could not be discovered, which indicates that MoO<sub>3</sub> and CoO have good dispersion in these supports. Consequently, MoO<sub>3</sub>, CoO, and compounds are well dispersed in the support.

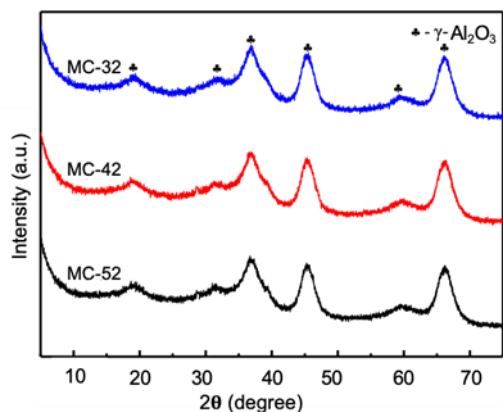


**Figure 2.** XRD patterns of the catalysts with different Mo amount.

The pore structure of catalysts with different Mo amount was characterized by N<sub>2</sub> adsorption-desorption measurements, and the results are summarized in Figure 3 and Table 2. Figure 3 shows that the isotherms of three catalysts with different Mo amount have an obvious H4-type hysteresis loop at P/P<sub>0</sub> ranging from 0.6 to 1.0, indicating that these catalysts exist mesoporous nature. The pore size distribution estimated by the Barrett-Joyner-Halenda (BJH) method reveals the mesoporous in the catalysts distributed between 9 and 12 nm, as seen in the part (B) of Figure 3. The BET surface area ( $S_{\text{BET}}$ ), pore volume, and average pore size of the mesoporous catalysts are shown in

Table 2. The BET surface area of catalysts has no changes when the Mo amount of catalysts rise. However, the pore volume and size of catalysts increase with the increase of the Mo amount of catalysts. In general, the larger the expected BET surface area, pore volume, and pore size of catalysts are, the better the HDS performance of catalysts are. Therefore, the MoO<sub>3</sub> amount is expected to be 4 wt.% due to the larger pore volume.

**Table 2.** Textural Properties of the Catalysts with Different Mo Content

Catalyst	BET surface area (m <sup>2</sup> /g)	Pore volume (cm <sup>3</sup> /g)	Average pore size (nm)
ML-52	242	0.58	9.5
ML-42	242	0.60	9.8
ML-32	243	0.60	9.9

### 3.1.2. Catalytic Test of Catalysts with Various Mo Content

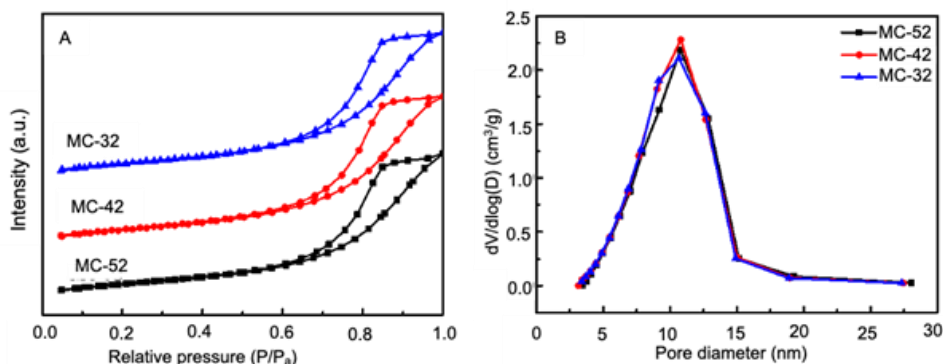
The catalytic performances of the three catalysts were tested using the dibenzothiophene of *n*-heptane as a model reaction, and the results are summarized in Figure 4. Under the experimental conditions, all of the three catalysts have over 90% of the HDS conversion ratio. When the amount of MoO<sub>3</sub> increases from 3 to 4 wt.%, the HDS conversion ratio has an obvious increase, which denotes that the activity metal Mo is useful for the HDS conversion ratio. However, the HDS conversion ratio has no distinct change when the MoO<sub>3</sub> amount increases from 4 to 5 wt.%. It implies that the excessive Mo amount is unable to improve the HDS activity. Moreover, the excessive Mo amount would increase the preparation cost of catalysts. Therefore, the best MoO<sub>3</sub> amount could be 4 wt.%, which is consistent with the characterization results of XRD and N<sub>2</sub> adsorption-desorption.

## 3.2. Effect of Co Content on the Performance of CoMo/Al<sub>2</sub>O<sub>3</sub>-MgO Catalysts

Based on the above results, the impacts of Co amount on the HDS performance of the CoMo/Al<sub>2</sub>O<sub>3</sub>-MgO catalyst with 4 wt.% of MoO<sub>3</sub> were investigated. The obtained catalysts are named MC-40, MC-41, MC-42, and MC-43, which stands for the mass content of loaded CoO is from 0 to 3%. In this section, the structure and pore properties of catalysts are first analyzed; then acidity and reducibility properties of catalysts are measured. Afterward, the sulfurized degree of catalysts is investigated. Finally, the HDS reactions are conducted to prove the properties of catalysts.

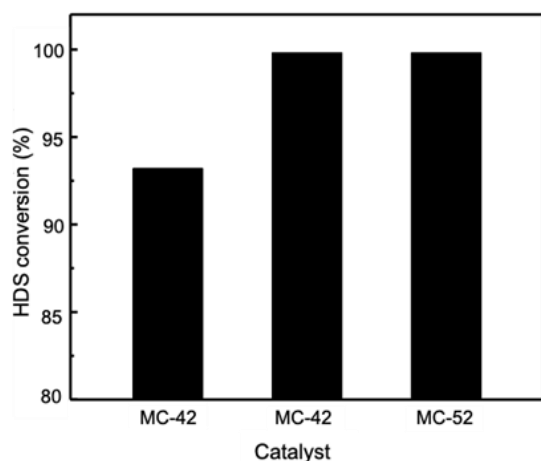
### 3.2.1. Structure and Pore Properties of Catalysts with Various Co Content

Figure 5 presents the XRD patterns of four catalysts with various amounts of Co. These four catalysts have similar XRD patterns, which suggests that the amounts of Co could not alter the phase structure of catalysts. These catalysts all have six characteristic peaks that all belong to the  $\gamma$ -Al<sub>2</sub>O<sub>3</sub> phase (PDF#29-0063), including (111), (220), (311), (400), (511), and (440) crystal planes. It could be known that the support is



**Figure 3.** N<sub>2</sub> adsorption-desorption isotherms (A) and pore size distribution curves of the catalysts with different Mo amount (B).

dominated by  $\gamma$ -Al<sub>2</sub>O<sub>3</sub> and little amount of MgO is well dispersed in the supports. The characteristic diffraction peaks of MoO<sub>3</sub> and CoO are unable to be found, demonstrating that MoO<sub>3</sub> and CoO also have well dispersion in the supports. The catalytic performance would be better when the desorption degree between the promoter and active metal is more uniform. Accordingly, these catalysts are prepared well.



**Figure 4.** Catalytic performance of the catalysts with different Mo amount.

The N<sub>2</sub> adsorption-desorption isotherms and pore size distribution of catalysts with different amounts of Co are displayed in Figure 6. The isotherms of all the catalysts exhibit a distinct H4-type hysteresis loop at P/P<sub>0</sub> ranging from 0.7 to 1.0, which indicates that these catalysts have mesoporous structure. The pore size distribution was estimated by the BJH method shown in Figure 6(B). It can be seen that the pore size distribution is between 9 and 12 nm.

The textural properties of the four catalysts are listed in Table 3. The BET surface area, pore volume, and pore size are slightly changed with the increase of Co content. When the amount of CoO is 1 wt.%, the BET surface area and pore volume are the largest. However, the BET surface area and pore size are the lowest when the amount of CoO is 2 wt.%. Comparing MC-42 and MC-43, the BET surface area, pore volume,

and pore size of catalysts with 3 wt.% of CoO are similar to that of the catalyst with 2 wt.% of CoO. Therefore, the amounts of CoO could not be determined by N<sub>2</sub> adsorption-desorption.

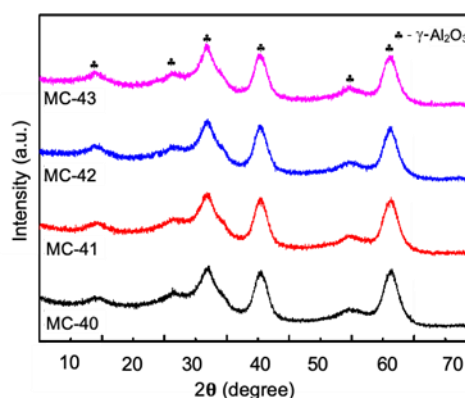


**Figure 5.** XRD patterns of the catalysts with different Co amount.

**Table 3.** Textural Properties of the Catalysts with Different Co Amount

Catalyst	BET surface area (m <sup>2</sup> /g)	Pore volume (cm <sup>3</sup> /g)	Average pore size (nm)
ML-40	248	0.62	10.0
ML-41	252	0.62	9.8
ML-42	243	0.60	9.8
ML-43	244	0.60	9.9

### 3.2.2. Acidity and Reducibility Properties of Catalysts with Various Co Content

The acidity properties of the catalysts were measured by NH<sub>3</sub>-TPD. From the NH<sub>3</sub>-TPD results given in Figure 7, we can observe that all of the catalysts show one desorption peaks centered at 220 ~ 350 °C, corresponding to medium-strong acid sites (Niwa and Katada, 2013). The activity, stability and service life of the catalyst are deeply affected by the acidity of the support surface (Hinnemann et al., 2008; Zhang et al., 2015). In terms of HDS catalysts, the acid center on the catalyst surface is the active center of catalytic reaction as well as carbon deposit center. The deposited degree of carbon increases as the

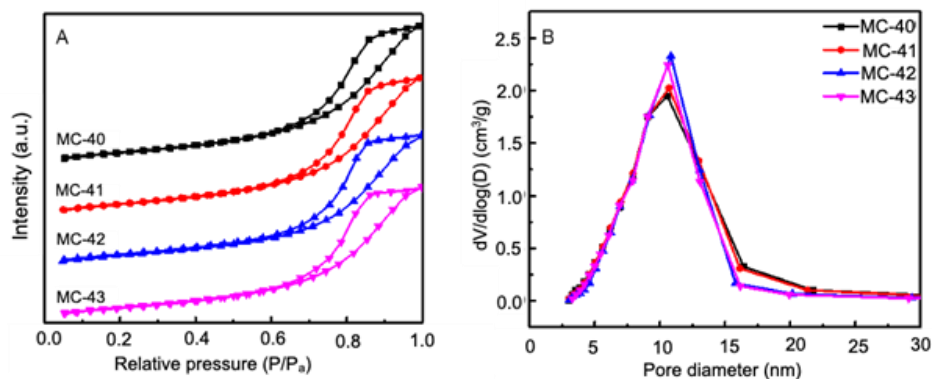


**Figure 6.** N<sub>2</sub> adsorption-desorption isotherms (A) and pore size distribution curves of the catalysts with different Co amount (B).

acidity of catalysts rise, which is harmful to the catalytic reaction. As a result, catalysts have an appropriate acidity that is helpful for catalytic reaction. The acid amount and strength of catalysts could be quantified via NH<sub>3</sub>-TPD, where the temperature of the NH<sub>3</sub> desorption peak represents the acid strength of the catalysts, and the desorption-peak area stands for the number of catalysts' acid sites. The desorption-peak areas have been normalized shown in upper right corner of Figure 7. It was found that amounts of catalysts' acid sites have an obvious increase when CoO content increases from 0 to 1 wt. %. Moreover, MC-43 containing 3 wt.% CoO has the highest number of catalysts' acid sites. However, catalysts with excessive acid strength have an opposite effect for the catalytic reaction. Consequently, the CoO content is expected to be 1 or 2 wt.% because MC-41 and MC-42 have a similar number of acid sites.

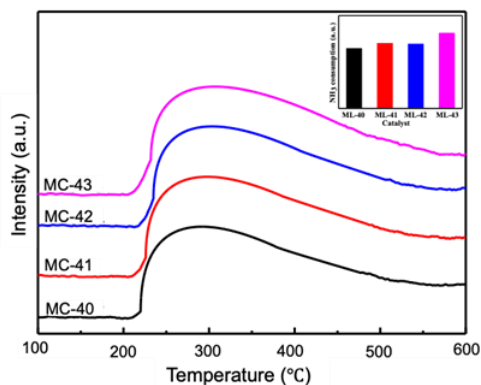


**Figure 7.** NH<sub>3</sub>-TPD curves of the catalysts with different Co amount.

The reducibility properties of four catalysts were assessed by H<sub>2</sub>-TPR, and the results are shown in Figure 8. All of catalysts show hydrogen consumption peaks centered at 460 ~ 570 °C and 700 ~ 950 °C, respectively. In detail, low-temperature reduction peaks are due to the reduction of Mo<sup>6+</sup> to Mo<sup>4+</sup> within the octahedral Mo species that have weak interactions with supports, while high-temperature reduction peaks are attributed to the deep reduction of all Mo species, including the reduction of Mo<sup>6+</sup> to Mo metal in the highly dispersed tetrahedral species

and Mo<sup>4+</sup> to Mo metal in octahedral species (Qu et al., 2003; Kumar et al., 2004). For Mo-based HDS catalysts, the weak interactions between active components and supports are conducive to the vulcanization of active components, which helps improve the stacking degree of active phase (MoS<sub>2</sub>) (Fan et al., 2007). When the CoO content is 2 wt.%, the temperature of low-temperature reduction peak (468 °C) and high-temperature reduction peak (832 °C) are both the lowest, indicating that MC-42 has the weakest interactions between the active metals and supports and highest stacking degree of MoS<sub>2</sub>. Furthermore, CoO and MoO<sub>3</sub> are more likely forming a mixed phase when interactions between the active metal and supports are weak (Chen et al., 2016). That is beneficial for the vulcanization of Co, Mo and the formation of the Co-Mo-S phase. Additionally, the activity of the corresponding catalysts is relatively higher, which is consistent with the results of the activity evaluation.

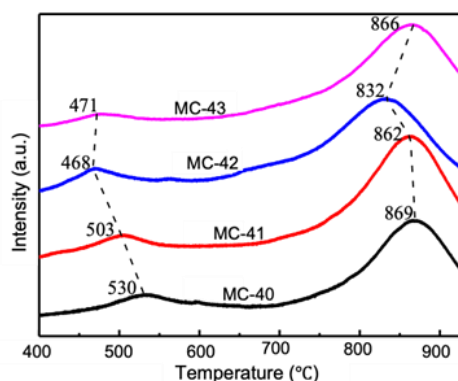


**Figure 8.** H<sub>2</sub>-TPR curves of the catalysts with different Co amount.

### 3.2.3. The Sulfurized Degree of Catalysts

The sulfidation behavior of Mo on the catalyst was investigated by XPS, and the results are summarized in Figure 9 and Table 4. A sulfide Mo species would be formed when catalysts are pre-sulfurized. The sulfidation degree of catalysts, as well as the formed Mo species, are closely related to the HDS activity and selectivity of the catalysts. The XPS spectra could be

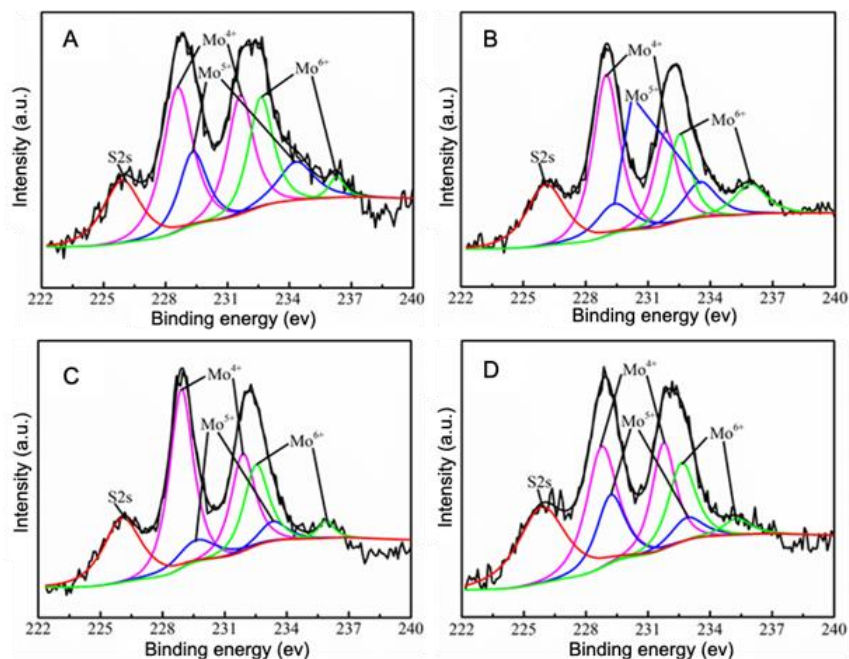


**Figure 9.** Mo3d and S2s XPS spectra of the sulfided catalysts: MC-40 (A), MC-41 (B), MC-42 (C), and ML-3 (D).

peak fitting according to the binding energy of different chemical valence of Mo species (Liu et al., 2014). Thus, the sulfidation degree of catalysts could be obtained by normalizing the peak areas of Mo species with different chemical valences. Table 4 shows that the degree of sulfidation first increases then decreases when the amounts of CoO increase from 0 to 3 wt.%. It is noted that MC-42 with 2 wt.% of CoO content has the highest degree of sulfidation (64.1%), indicating that an appropriate amount of Co could improve the degree of catalysts' sulfidation. The higher the degree of vulcanization is, the more MoS<sub>2</sub> lamellar crystals could be formed after vulcanization, which is helpful for HDS reaction. However, it would reduce the degree of catalysts' sulfurization when the Co content is over-dose because excess Co may exist as a separate sulfide, which may cause the active sites covered or blocked resulting in the decrease of catalyst activity (Chen et al., 2016). Consequently, the amounts of CoO are expected to be 2 wt.%.

**Table 4.** XPS Characterization Results of the Sulfided Catalysts

Catalyst	Mo <sup>4+</sup> (%)	Mo <sup>5+</sup> (%)	Mo <sup>6+</sup> (%)	Mo <sub>sulfidation</sub> (%)
MC-40	45.80	21.14	18.60	53.5
MC-41	46.28	16.09	20.64	55.8
MC-42	51.77	11.07	17.87	64.1
MC-43	41.46	17.77	17.03	54.4

### 3.2.4. Catalytic Tests of Catalysts with Different Co Content

The catalytic performances of the four catalysts are tested using the dibenzothiophene of *n*-heptane as a model reaction, and the results are summarized in Figure 10. Under the same reaction conditions, the catalysts containing CoO and MoO<sub>3</sub> have better catalytic performances than those with the only

MoO<sub>3</sub>, which indicates that the addition of Co greatly contributes to HDS reaction performance. When the amount of CoO increases from 1 to 3 wt.%, the HDS conversion grow first then remain stable, which revealed that the appropriate amounts of Co could help improve catalysts' activity. However, when the amounts Co in catalysts are excessive, it could not further promote HDS conversion, as well as increases the preparation cost of catalysts. Therefore, the amounts of CoO in catalysts are designed to be 2 wt.%.

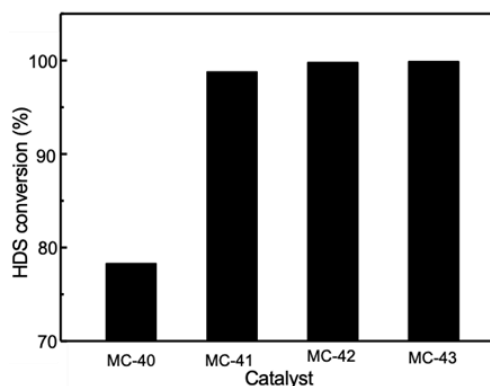


**Figure 10.** Catalytic performance of catalysts with different Co amount.

### 3.3. Optimization of HDS Reaction Conditions for CoMo/Al<sub>2</sub>O<sub>3</sub>-MgO Catalysts

The reaction conditions could also greatly affect selectivity and activity of the catalyst, so the reaction condition of HDS, including temperature, the pressure of hydrogen (H<sub>2</sub>), the volume ratio of H/Oil, and LHSV, are optimized and the results

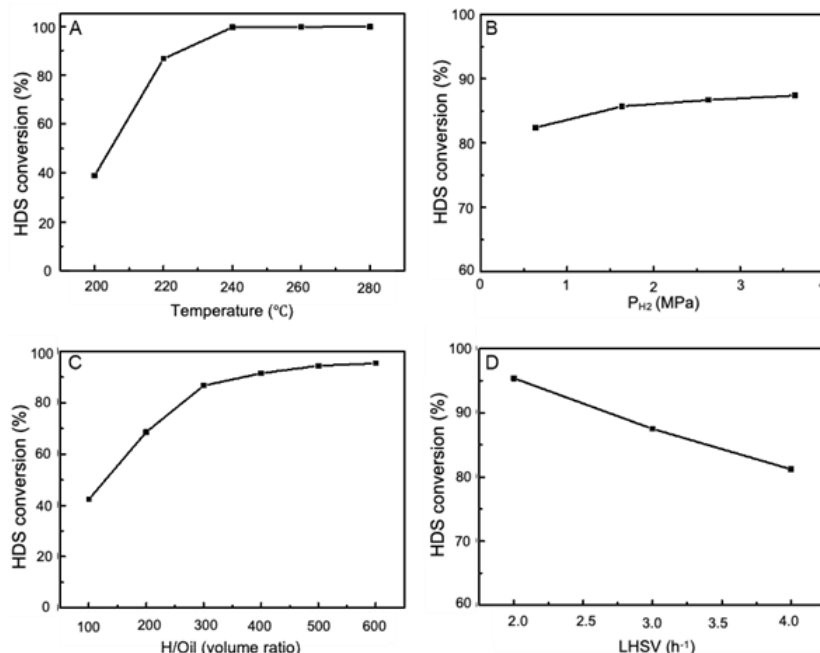


**Figure 11.** Effects of reaction conditions on the conversion of DBT: temperature (A), pressure of H<sub>2</sub> (B), volume ratio of H/Oil (C), and LHSV (D).

are summarized in Figure 11. It is known that the effect of reaction temperature on HDS is in accordance with the Arrhenius equation. As the reaction temperature increases, the reaction rate constant also grows, which is beneficial to accelerate the reaction speed. Figure 11(A) shows that the DBT conversion rate has an obvious increase when reaction temperature grows from 200 to 240 °C, implying that reaction temperature is mainly affected by reaction thermodynamics, and the increasing reaction temperature is helpful to the HDS. When the reaction temperature is over 240 °C, the conversion of DBT has no significant alteration with the increase of reaction temperature, which is similar to the results observed by Kabe et al. (1993). Consequently, the reaction temperature is chosen to be 240 °C.

The effect of H<sub>2</sub> pressure on the HDS reaction is presented in Figure 11(B). The conversion rate of DBT is positively related to the hydrogen partial pressure. In detail, DBT mainly exists in a gas-phase form within a certain pressure range. When the hydrogen partial pressure increases during the HDS process, it could reduce the rate of carbon deposits on the catalyst surface area, thereby increasing its service life. Whereas, the conversion of DBT increases slowly when the reaction hydrogen partial pressure exceeds 2.6 MPa. The reason is that excessive reaction pressure would result in the appearance of a liquid phase in the reaction system (Wang et al., 2012; Guo et al., 2016). When catalysts' surface was covered by the liquid, it would be easily formed a liquid film with a certain resistance. As a result, it is difficult for hydrogen to diffuse in the catalyst, which reduces the reaction rate. Moreover, excessive pressure will increase investment in the reaction equipment. Thus, the optimal hydrogen partial pressure is 2.6 MPa, that is, the total reaction pressure is 4.0 MPa.

Figure 11(C) shows the effect of the H/Oil volume ratio on the DBT conversion. In the industrial hydro refining process, the consumption of circulating hydrogen is affected by the H/Oil volume ratio. Underachieving the same desulfurization effect, the smaller the H/Oil volume ratio is, the smaller the consumption of circulating hydrogen, which can save a lot of energy consumption (Dong et al., 2006). When the volume ratio H/Oil raises from 100 to 300, the conversion rate of DBT has a significant rise. The reason is that increasing the H/Oil volume ratio can increase the hydrogen partial pressure during the reaction process so that the raw material is easier vaporized (Dong et al., 2006). As a result, the thickness of the liquid film on the catalyst surface is reduced, thereby improving the conversion rate of DBT. However, the conversion rate of DBT slowly grows when the H/Oil volume ratio exceeds 300. This is because the residence time of reactants in the catalyst surface is decreased when the H/Oil volume ratio is too high, which may result in the reactants without completely reacting. Additionally, the excessive H/Oil volume ratio increases hydrogen consumption, that is, reaction cost. Therefore, the optimal H/Oil volume ratio is 300.

Alterations in LHSV reveal the changes in contact time between reactants and catalyst (Li et al., 2003). In Figure 11(D), LHSV has a negative correlation with the conversion rate of DBT, that is, the conversion rate of DBT decreases with the increase of LHSV. When the LHSV is low, the contact time between the reactant and catalyst increases, at the same time, the hydrogen consumption grows as well, which enhances the HDS process. On the other hand, when the LHSV is high, the contact time between the reactants and the catalyst is correspondingly shortened. Moreover, the sulfide preferentially ac-

cumulates on the catalyst surface, thereby accelerating carbon deposition on the catalyst surface, leading to a decrease in the conversion rate of DBT. Hence, the optimal LHSV is  $2.0 \text{ h}^{-1}$ .

#### 4. Conclusions

In summary, a series of CoMo/Al<sub>2</sub>O<sub>3</sub>-MgO named MC-xy were prepared by using the composite oxides of MgAl-hydrotalcite and alumina as supports via an incipient-wetness impregnation method. Moreover, their catalytic performances were evaluated by using dibenzothiophene (DBT) in *n*-heptane solution as a raw material in a fix-bed reactor. Furthermore, the effects of activity metal (Mo) and promoter (Co) on the catalysts were assessed to gain the optimal amounts of MoO<sub>3</sub> and CoO. Finally, the reaction conditions are optimized through the HDS process.

The activity metal Mo could improve the catalytic performance of catalysts, while excessive additivity not only could not improve the catalysts' performance but also increase the preparation cost of catalysts. The results of XRD, nitrogen adsorption-desorption, and the catalytic test show that the optimal amounts of MoO<sub>3</sub> are 4 wt.%. Similarly, an appropriate addition of Co could also improve catalysts' performance. Combining the results from XRD, nitrogen adsorption-desorption, NH<sub>3</sub>-TPD, H<sub>2</sub>-TPR, and XPS, we can gain the optimal amounts of CoO (2 wt.%), which is consistent with the results of the catalytic test. Finally, using the catalysts with 4 wt.% of MoO<sub>3</sub> and 2 wt.% of CoO to optimize the reaction conditions, the optimal process conditions are determined, including reaction temperature of 240 °C, total reaction pressure of 4.0 MPa, the H/Oil volume ratio of 300, and LHSV of  $2.0 \text{ h}^{-1}$ , as well as gain the desulfurization rate of 99.8%.

**Acknowledgments.** The authors gratefully acknowledge the funding from National Natural Science Foundation of China (grants 22178059 and 22208054), and Natural Science Foundation of Fujian Province, China (grant 2020J01513).

#### References

- Ancheyta, J., Rana, M.S. and Furimsky, E. (2005). Hydroprocessing of heavy petroleum feeds: Tutorial. *Catalysis today*, 109(1-4), 3-15. <https://doi.org/10.1016/j.cattod.2005.08.025>
- Breysse, M., Afanasiev, P., Geantet, C. and Vrinat, M. (2003a). Overview of support effects in hydrotreating catalysts. *Catalysis Today*, 86(1-4), 5-16. [https://doi.org/10.1016/S0920-5861\(03\)00400-0](https://doi.org/10.1016/S0920-5861(03)00400-0)
- Breysse, M., Djega-Mariadassou, G., Pessayre, S., Geantet, C., Vrinat, M., Pérot, G. and Lemaire, M. (2003b). Deep desulfurization: reactions, catalysts and technological challenges. *Catalysis Today*, 84(3-4), 129-138. [https://doi.org/10.1016/S0920-5861\(03\)00266-9](https://doi.org/10.1016/S0920-5861(03)00266-9)
- Caloch, B., Rana, M.S. and Ancheyta, J. (2004). Improved hydrogenolysis (C-S, C-M) function with basic supported hydrodesulfurization catalysts. *Catalysis Today*, 98(1-2), 91-98. <https://doi.org/10.1016/j.cattod.2004.07.023>
- Chen, S., Long, X., Chen, W.S. and Nie, H. (2016). Influence of the Promoter of Co-Mo/ $\gamma$ -Al<sub>2</sub>O<sub>3</sub> on the Hydrogen Consumption in Hydrodesulfurization Reaction. *Acta Petrolei Sinica (Petroleum Processing Section)*, 32(2), 244-253. <https://doi.org/10.3969/j.issn.1001-8719.2016.02.004>
- Dong, Z.G., Yu, X.Z., Ren, X.Q., Wang, J. and Wang, Y.R. (2006). Studies on the kinetics of the hydrodesulfurization of dibenzothiophene over a commercial NiW/Al<sub>2</sub>O<sub>3</sub> catalyst. *Journal of Chemical Engineering of Chinese University*, 20(3), 362-367. [https://doi.org/10.3969/j.issn.1003-9015\(2006\)03-0362-06](https://doi.org/10.3969/j.issn.1003-9015(2006)03-0362-06)
- Eijsbouts, S., Mayo, S.W. and Fujita, K. (2007). Unsupported transition metal sulfide catalysts: From fundamentals to industrial application. *Applied Catalysis A: General*, 322, 58-66. <https://doi.org/10.1016/j.apcata.2007.01.008>
- Fan, Y., Bao, X.J., Wang, H., Chen, C.F. and Shi, G. (2007). A surfactant-assisted hydrothermal deposition method for preparing highly dispersed W/ $\gamma$ -Al<sub>2</sub>O<sub>3</sub> hydrodenitrogenation catalyst. *Journal of Catalysis*, 245(2), 477-481. <https://doi.org/10.1016/j.jcat.2006.11.003>
- Fan, Y., Xiao, H., Shi, G., Liu, H.Y., Qian, Y., Wang, T.H., Gong, G.B. and Bao, X.J. (2011). Citric acid-assisted hydrothermal method for preparing NiW/USY-Al<sub>2</sub>O<sub>3</sub> ultradeep hydrodesulfurization catalysts. *Journal of Catalysis*, 279(1), 27-35. <https://doi.org/10.1016/j.jcat.2010.12.014>
- Fujikawa, T., Kimura, H., Kiriya, K. and Hagiwara, K. (2006). Development of ultra-deep HDS catalyst for production of clean diesel fuels. *Catalysis Today*, 111(3-4), 188-193. <https://doi.org/10.1016/j.cattod.2005.10.024>
- Guo, Y.Q., Liu, D., Gao, Y., Ao, H.W., Wang, S.B., Li, Q.Y. and Yan, F. (2016). Study of Process Condition and Kinetics of Hydrodesulfurization of Low-Quality Diesel Oil. *Journal of Liaoning University of Petroleum and Chemical Technology*, 36(3), 15-19. <https://doi.org/10.3969/j.issn.1672-6952.2016.03.004>
- Hamiye, R., Lancelot, C., Blanchard, P., Toufaily, J., Hamieh, T. and Lamonier, C. (2017). Diesel HDS performance of alumina supported CoMoP catalysts modified by sulfone molecules produced by ODS process. *Fuel*, 210, 666-673. <https://doi.org/10.1016/j.fuel.2017.09.025>
- Hensen, E.D., De Beer, V.H.J., Van Veen, J.A.R. and Van Santen, R.A. (2002). A refinement on the notion of type I and II (Co) MoS phases in hydrotreating catalysts. *Catalysis Letters*, 84(1), 59-67. <https://doi.org/10.1023/A:1021024617582>
- Hensen, E.J.M., van der Meer, Y., van Veen, J.A.R. and Niemantsverdriet, J.W. (2007). Insight into the formation of the active phases in supported NiW hydrotreating catalysts. *Applied Catalysis A: General*, 322, 16-32. <https://doi.org/10.1016/j.apcata.2007.01.003>
- Hinnemann, B., Moses, P.G. and Nørskov, J.K. (2008). Recent density functional studies of hydrodesulfurization catalysts: insight into structure and mechanism. *Journal of Physics: Condensed Matter*, 20(6), 064236. <https://doi.org/10.1088/0953-8984/20/6/064236>
- Ho, T.C. (2004). Deep HDS of diesel fuel: chemistry and catalysis. *Catalysis Today*, 98(1-2), 3-18. <https://doi.org/10.1016/j.cattod.2004.07.048>
- Kabe, T., Ishihara, A. and Zhang, Q. (1993). Deep desulfurization of light oil. Part 2: Hydrodesulfurization of dibenzothiophene, 4-methylthiophene and 4, 6-dimethylthiophene. *Applied Catalysis A: General*, 97(1), L1-L9. [https://doi.org/10.1016/0926-860X\(93\)80059-Y](https://doi.org/10.1016/0926-860X(93)80059-Y)
- Ke, X.M. and Wang, L.M. (2016). Analysis of the fifth stage of gasoline and diesel quality upgrade roadmap in China. *International Petroleum Economics*, (5), 21-27. <https://doi.org/10.3969/j.issn.1004-7298.2016.05.004>
- Klicpera, T. and Zdražil, M. (2002). Preparation of high-activity MgO-supported Co-Mo and Ni-Mo sulfide hydrodesulfurization catalysts. *Journal of Catalysis*, 206(2), 314-320. <https://doi.org/10.1006/jcat.2001.3488>
- Klimova, T., Casados, D.S. and Ramirez, J. (1998). New selective Mo and NiMo HDS catalysts supported on Al<sub>2</sub>O<sub>3</sub>-MgO (x) mixed oxides. *Catalysis Today*, 43(1-2), 135-146. [https://doi.org/10.1016/S0920-5861\(98\)00142-4](https://doi.org/10.1016/S0920-5861(98)00142-4)
- Kouzu, M., Kuriki, Y., Hamdy, F., Sakanishi, K., Sugimoto, Y. and

- Saito, I. (2004). Catalytic potential of carbon-supported NiMo-sulfide for ultra-deep hydrodesulfurization of diesel fuel. *Applied Catalysis A: General*, 265(1), 61-67. <https://doi.org/10.1016/j.apcata.2004.01.003>
- Kumar, M., Aberuagba, F., Gupta, J.K., Rawat, K.S., Sharma, L.D. and Dhar, G.M. (2004). Temperature-programmed reduction and acidic properties of molybdenum supported on MgO–Al<sub>2</sub>O<sub>3</sub> and their correlation with catalytic activity. *Journal of Molecular Catalysis A: Chemical*, 213(2), 217-223. <https://doi.org/10.1016/j.molcata.2003.12.005>
- Lauritsen, J.V., Helveg, S., Lægsgaard, E., Stensgaard, I., Clausen, B. S., Topsøe, H. and Besenbacher, F. (2001). Atomic-scale structure of Co–Mo–S nanoclusters in hydrotreating catalysts. *Journal of Catalysis*, 197(1), 1-5. <https://doi.org/10.1006/jcat.2000.3088>
- Lauritsen, J.V., Kibsgaard, J., Olesen, G.H., Moses, P.G., Hinnemann, B., Helveg, S., Nørskov, J.K., Clausen, B.S., Topsøe, H., Lægsgaard, E. and Besenbacher, F. (2007). Location and coordination of promoter atoms in Co- and Ni-promoted MoS<sub>2</sub>-based hydrotreating catalysts. *Journal of Catalysis*, 249(2), 220-233. <https://doi.org/10.1016/j.jcat.2007.04.013>
- Li, L. (2016). The course of China's gasoline and diesel quality upgrading and its prospect. *Petroleum and Petrochemical Today*, 24(7), 23-28. <https://doi.org/cnki:sun:sygd.0.2016-07-005>
- Li, X., Wang, A.J., Sun, Z.C., Li, C. and Hu, Y.K. (2003). Study on Hydrodesulfurization Kinetics of Dibenzothiophene over Ni-W Sulfides Supported by Siliceous MCM-41. *Acta Petrolei Sinica (Petroleum Processing Section)*, 19(4), 1-7. [https://doi.org/1001-8719\(2003\)04-0001-07](https://doi.org/1001-8719(2003)04-0001-07)
- Liu, B., Chai, Y.M., Li, Y.P., Wang, A.J., Liu, Y.Q. and Liu, C.G. (2014). Effect of sulfidation atmosphere on the performance of the CoMo/γ-Al<sub>2</sub>O<sub>3</sub> catalysts in hydrodesulfurization of FCC gasoline. *Applied Catalysis A: General*, 471, 70-79. <https://doi.org/10.1016/j.apcata.2013.11.017>
- Niwa, M. and Katada, N. (2013). New Method for the Temperature-Programmed Desorption (TPD) of Ammonia Experiment for Characterization of Zeolite Acidity: A Review. *The Chemical Record*, 13(5), 432-455. <https://doi.org/10.1002/tcr.201300009>
- Oyama, S.T., Gott, T., Zhao, H. and Lee, Y.K. (2009). Transition metal phosphide hydroprocessing catalysts: A review. *Catalysis Today*, 143(1-2), 94-107. <https://doi.org/10.1016/j.cattod.2008.09.019>
- Peña, L., Valencia, D. and Klimova, T. (2014). CoMo/SBA-15 catalysts prepared with EDTA and citric acid and their performance in hydrodesulfurization of dibenzothiophene. *Applied Catalysis B: Environmental*, 147, 879-887. <https://doi.org/10.1016/j.apcatb.2013.11.019>
- Qiu, L. and Xu, G. (2010). Peak overlaps and corresponding solutions in the X-ray photoelectron spectroscopic study of hydrodesulfurization catalysts. *Applied surface science*, 256(11), 3413-3417. <https://doi.org/10.1016/j.apsusc.2009.12.043>
- Qu, L.L., Zhang, W.P., Kooyman, P.J. and Prins, R. (2003). MAS NMR, TPR, and TEM studies of the interaction of NiMo with alumina and silica–alumina supports. *Journal of Catalysis*, 215(1), 7-13. [https://doi.org/10.1016/S0021-9517\(02\)00181-1](https://doi.org/10.1016/S0021-9517(02)00181-1)
- Rana, M.S., Huidobro, M.L., Ancheyta, J. and Gómez, M.T. (2005). Effect of support composition on hydrogenolysis of thiophene and Maya crude. *Catalysis today*, 107-108, 346-354. <https://doi.org/10.1016/j.cattod.2005.07.029>
- Song, C. (2003). An overview of new approaches to deep desulfurization for ultra-clean gasoline, diesel fuel and jet fuel. *Catalysis today*, 86(1-4), 211-263. [https://doi.org/10.1016/S0920-5861\(03\)00412-7](https://doi.org/10.1016/S0920-5861(03)00412-7)
- Sun, M., Nelson, A.E. and Adjaye, J. (2004). A DFT study of WS<sub>2</sub>, NiWS, and CoWS hydrotreating catalysts: energetics and surface structures. *Journal of catalysis*, 226(1), 41-53. <https://doi.org/10.1016/j.jcat.2004.04.023>
- Topsøe, H., Clausen, B.S. and Massoth, F.E. (1996). *Catalysis Science and Technology*. JR Anderson and M. Boudard'. Springer, Berlin.
- Topsøe, H., Clausen, B.S., Candia, R., Wivel, C. and Mørup, S. (1981). In situ Mössbauer emission spectroscopy studies of unsupported and supported sulfided Co-Mo hydrodesulfurization catalysts: Evidence for and nature of a Co-Mo-S phase. *Journal of catalysis*, 68(2), 433-452. [https://doi.org/10.1016/0021-9517\(81\)90114-7](https://doi.org/10.1016/0021-9517(81)90114-7)
- Trejo, F., Rana, M.S. and Ancheyta, J. (2008). CoMo/MgO–Al<sub>2</sub>O<sub>3</sub> supported catalysts: An alternative approach to prepare HDS catalysts. *Catalysis Today*, 130(2-4), 327-336. <https://doi.org/10.1016/j.cattod.2007.10.105>
- Vissenberg, M.J., Van der Meer, Y., Hensen, E.J.M., De Beer, V.H.J., Van Der Kraan, A.M., Van Santen, R.A. and Van Veen, J.A.R. (2001). The effect of support interaction on the sulfidability of Al<sub>2</sub>O<sub>3</sub>- and TiO<sub>2</sub>-supported CoW and NiW hydrodesulfurization catalysts. *Journal of Catalysis*, 198(2), 151-163. <https://doi.org/10.1006/jcat.2000.3132>
- Wagner, C.D., Riggs, W.M., Davis, L.E., Moulder, J.F. and Muilenberg, G.E. (1979). *Handbook of X-ray photoelectron spectroscopy: a reference book of standard spectra for identification and interpretation of XPS data*. Perkin-Elmer Corporation Physical Electronics Division, Eden Prairie, Minnesota, USA. <https://doi.org/10.1002/S IA.740030412>
- Wang, J.Y., Lu, R.X., Du, W.B., Chen, S.H. and Zeng, C.Y. (2012). Kinetics of hydrodesulfurization of diesel over Ni-Mo/TiO<sub>2</sub>-Al<sub>2</sub>O<sub>3</sub> catalyst. *Petrochemical Technology*, 41(11), 1277-1281. <https://doi.org/10.1016/j.matlet.2011.08.044>
- Yue, Y.Y., Zheng, X.G., Kang, Y., Bai, Z.S., Yuan, P., Zhu, H.B. and Bao, X.J. (2018). Preparation of Mo/Al<sub>2</sub>O<sub>3</sub>-MgO catalysts from MgAl-hydrotalcite and their hydrogenation desulfurization performance. *CIESC Journal*, 69(1), 405-413. <https://doi.org/10.11949/j.issn.0438-1157.20170727>
- Zhang, Y., Wang, J.F., Zhao, D.Z., Yuan, S.H., Zhang, C. and Guan, Y.M. (2015). The modification of pore structure and acidity of γ-Al<sub>2</sub>O<sub>3</sub> support. *Petrochemical Technology and Application*, 33(4), 366-370. [https://doi.org/1009-0045\(2015\)04-0366-05](https://doi.org/1009-0045(2015)04-0366-05)
- Zuo, D., Li, D., Nie, H., Shi, Y., Lacroix, M. and Vrinat, M. (2004). Acid-base properties of NiW/Al<sub>2</sub>O<sub>3</sub> sulfided catalysts: relationship with hydrogenation, isomerization and hydrodesulfurization reactions. *Journal of Molecular Catalysis A: Chemical*, 211(1-2), 179-189. <https://doi.org/10.1016/j.molcata.2003.10.018>